www.lajss.org
Latin American Journal of Solids and Structures 2 (2005) 103–112

Weld investigations by 3D analyses of Charpy V-notch specimens

Viggo Tvergaard[a,*] and Alan Needleman[b]

[a]Department of Mechanical Engineering, Technical University of Denmark, DK-2800 Kgs. Lyngby, Denmark
[b]Brown University, Division of Engineering, Providence, RI 02912, USA

Abstract

The Charpy impact test is a standard procedure for determining the ductile-brittle transition in welds. The predictions of such tests have been investigated by full three dimensional transient analyses of Charpy V-notch specimens. The material response is characterised by an elastic-viscoplastic constitutive relation for a porous plastic solid, accounting for adiabatic heating due to plastic dissipation and the resulting thermal softening. The onset of cleavage is taken to occur when the average of the maximum principal stress over a specified volume attains a critical value. Typically, the material parameters in the weld material differ from those in the base material, and the heat affected zone (HAZ) tends to be more brittle than the other material regions. The effect of weld strength undermatch or overmatch is an important issue. Some specimens, for which the notched surface is rotated relative to the surface of the test piece, have so complex geometry that only a full 3D analysis is able to account for the interaction of failure in the three different material regions, whereas other specimens can be approximated in terms of a planar analysis

1 Introduction

The application of the micromechanically based elastic-viscoplastic material model, accounting for ductile failure by the nucleation and growth of voids to coalescence as well as for brittle cleavage failure in analyses of the ductile-brittle transition in Charpy V-notch specimens, has been initiated in planar analyses by Tvergaard and Needleman [13, 14]. Subsequently, full 3D analyses for homogeneous specimens have been carried out [6], and planar analyses have been used in a detailed investigation of size effects in the Charpy test [1]. The general understanding of this test for characterizing the ductile-brittle transition in steels has been discussed by Ritchie [8] and in a recent book celebrating the hundredth anniversary of the test [3]. According to European standards for destructive tests on welds in metallic materials, Charpy specimens are cut out so that they are perpendicular to the weld and parallel to the surface of the test piece. The specimen can be cut at various depths below the surface of the test piece, and the notch face of the impact test specimen is chosen either parallel or perpendicular to the surface of the

* Corresponding author E-mail: viggo@mek.dtu.dk
Received 06 December 2004
From *Recent Developments in the Modelling of Rupture in Solids Conference*, ed. A. Benallal & S.P.B. Proença.

test piece, with the location of the notch measured relative to the center of the weld, so that the notch can be in the base material, in the weld material, or in the heat affected zone (HAZ).

When the notched face of the impact test specimen is parallel to the surface of the test piece, the geometry can be approximated by a planar analysis to investigate how the energy absorption and the fracture behavior depend on the location of the notch relative to details of the weld geometry. A study for plane strain conditions has been carried out by the authors [16], accounting for the difference in flow strength and hardening behavior of the base material, the weld material and the HAZ. These planar analyses have shown a strong sensitivity of the work of fracture to the location of the notch relative to the weld, with the most brittle behavior for a notch close to the narrow heat affected zone. For the same type of specimen geometry, relative to the weld, a few three dimensional analyses have been presented in [17].

The present paper will focus on discussing full 3D analyses for Charpy V-notch tests cut out of welded joints [18]. Even for the specimens where the weld material geometry allows for a planar analysis, it will be shown that due to the specimen geometry three dimensional effects play an important role in the prediction of the failure evolution. Also some results of planar analyses will be included in the present discussion.

2 Problem formulation and material model

A convected coordinate Lagrangian formulation is used with the dynamic principle of virtual work written as

$$\int_V \tau^{ij}\delta\eta_{ij}dV = \int_S T^i\delta u_i dS - \int_V \rho\frac{\partial^2 u^i}{\partial t^2}\delta u_i dV \tag{1}$$

with

$$T^i = \left(\tau^{ij} + \tau^{kj}u^i_{,k}\right)\nu_j \tag{2}$$

$$\eta_{ij} = \frac{1}{2}\left(u_{i,j} + u_{j,i} + u^k_{,i}u_{k,j}\right) \tag{3}$$

Here, τ^{ij} are the contravariant components of Kirchhoff stress on the deformed coordinates, σ^{ij} are the Cauchy stress components, and $\tau^{ij} = J\sigma^{ij}$ with the ratio J of current to reference volumes. The covariant components of the reference surface normal and displacement vectors, are ν_j and u_j , ρ is the mass density, V and S are the volume and surface of the body in the reference configuration, and $(\,)_{,i}$ denotes covariant differentiation in the reference frame.

A standard Charpy V-notch specimen is analyzed, with overall length 55 mm, width 10 mm, notch depth 2 mm, notch radius 0.25 mm, notch angle 22.5° and 40 mm distance between supports. The specimen thickness is 10 mm. The geometry of the specimen and weld configuration is illustrated in Fig. 1. The boundary conditions are

$$\dot{u}_1 = 0 \quad \text{on the supports} \tag{4}$$

and

$$\dot{u}_1 = -V(t) \quad \text{on the striker-specimen interface} \tag{5}$$

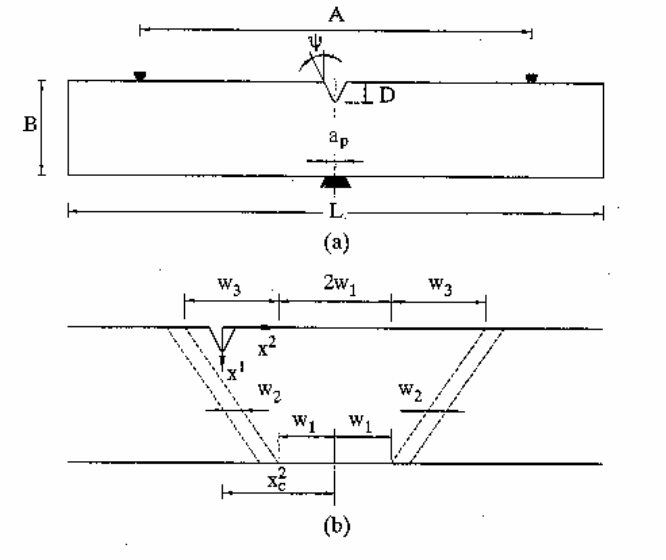

Figure 1: (a) Geometry of the Charpy specimen. (b) Geometry of the weld.

The striker is taken to contact the specimen on a $2\,mm \times 10\,mm$ area along the specimen axis ($a_p = 2\,mm$ in Fig. 1a). The impact is represented by the imposed velocity

$$V(t) = \begin{cases} V_1 t/t_r & for \quad t > t_r \\ V_1 & for \quad t > t_r \end{cases} \tag{6}$$

where $V_1 = 5\ m/s$ and $t_r = 20\ \mu s$. All other external surfaces are traction free. At $t = 0$, the specimen is assumed to be stress free (so that any effect of residual stresses is ignored) and to have the uniform initial temperature Θ_{init} .

The constitutive framework is the modified Gurson model. The rate of deformation tensor written as the sum of an elastic part, $\mathbf{d^e}$, a viscoplastic part, $\mathbf{d^p}$, and a part due to thermal straining, $\mathbf{d^\Theta}$, so that

$$\mathbf{d} = \mathbf{d^e} + \mathbf{d^p} + \mathbf{d^\Theta} \tag{7}$$

with

$$\mathbf{d^e} = \mathbf{L}^{-1} : \hat{\boldsymbol{\sigma}} \quad , \quad \mathbf{d^\Theta} = \alpha\dot{\Theta}\mathbf{I} \tag{8}$$

Here, small elastic strains are assumed, $\hat{\boldsymbol{\sigma}}$ is the Jaumann rate of Cauchy stress, Θ is the temperature, α is the thermal expansion coefficient, $\mathbf{A} : \mathbf{B} = A^{ij}B_{ji}$ and $\mathbf{L}$ is the tensor of isotropic elastic moduli. The properties are chosen to have representative values for steel; $E = 202\ GPa$, $\nu = 0.3$ and $\alpha = 1 \times 10^{-5}/^oK$.

The flow potential is, Gurson [5],

$$\Phi = \frac{\sigma_e^2}{\bar{\sigma}^2} + 2q_1 f^* \cosh\left(\frac{3q_2\sigma_h}{2\bar{\sigma}}\right) - 1 - (q_1 f^*)^2 = 0 \tag{9}$$

and $\mathbf{d^p}$ is given in Pan *et al.* [7]. The parameters $q_1 = 1.25$ and $q_2 = 1.0$ are introduced in Tvergaard [9, 10], f is the void volume fraction, $\bar{\sigma}$ is the matrix flow strength, and σ_e , σ_h are the macroscopic Mises stress, and hydrostatic tension, respectively.

The function f^* , Tvergaard and Needleman [12], accounts for the effects of rapid void coalescence at failure.

$$f^* = \begin{cases} f & f < f_c \\ f_c + (1/q_1 - f_c)\,(f - f_c)\,/\,(f_f - f_c) & f \geq f_c \end{cases} \tag{10}$$

where the values $f_c = 0.12$ and $f_f = 0.25$ are used. Background on the basis for the choice of parameter values in the Gurson model is given by Tvergaard [11].

The matrix plastic strain rate, $\dot{\bar{\varepsilon}}$, is given by

$$\dot{\bar{\varepsilon}} = \dot{\varepsilon}_0 \left[\frac{\bar{\sigma}}{g\,(\bar{\varepsilon}, \Theta)}\right]^{1/m} , \quad g\,(\bar{\varepsilon}, \Theta) = \sigma_0 G\,(\Theta)\,[1 + \bar{\varepsilon}/\varepsilon_0]^N \tag{11}$$

with $\bar{\varepsilon} = \int \dot{\bar{\varepsilon}} dt$, $\varepsilon_0 = \sigma_0/E$ and Θ_0 a reference temperature. In all cases, $\dot{\varepsilon}_0 = 10^3/s$ and $m = 0.01$.

Calculations are carried out for a set of material properties representative of an HY100 steel and an exponential temperature-dependence of the flow strength is assumed,

$$G\,(\Theta) = 1 + b \exp\left(-c\,[\Theta_0 - 273]\right)\left[\exp\left(-c\,[\Theta - \Theta_0]\right) - 1\right] \tag{12}$$

with $b = 0.1406$ and $c = 0.00793/^oK$. In (10), Θ and Θ_0 are in ^oK and $\Theta_0 = 293^oK$. The flow strength values used are chosen to fit data of Gray and Chen [4] and are $\sigma_0^{base} = 790\,MPa$, $\sigma_0^{weld} = 890\ MPa$ and $\sigma_0^{HAZ} = 1140\,MPa$. The corresponding strain hardening exponents are taken to be $N = 0.066$, $N = 0.057$ and $N = 0.041$, respectively.

Under the assumed adiabatic conditions, the balance of energy gives

$$\rho c_p \frac{\partial \Theta}{\partial t} = \chi \boldsymbol{\tau} : \mathbf{d^p} \tag{13}$$

where $\chi = 0.9$, $\rho = 7600\ kg/m^3$ and $c_p = 465\ J/\,(kg^oK)$.

The rate of increase of the void volume fraction is given by

$$\dot{f} = (1 - f)\,\mathbf{d^p} : \mathbf{I} + \mathcal{D}\dot{\bar{\varepsilon}} \tag{14}$$

with void nucleation taken to follow a normal distribution, Chu and Needleman [2], so that

$$\mathcal{D} = \frac{f_N}{s_N\sqrt{2\pi}} \exp\left[-\frac{1}{2}\left(\frac{\bar{\varepsilon} - \varepsilon_N}{s_N}\right)^2\right] \tag{15}$$

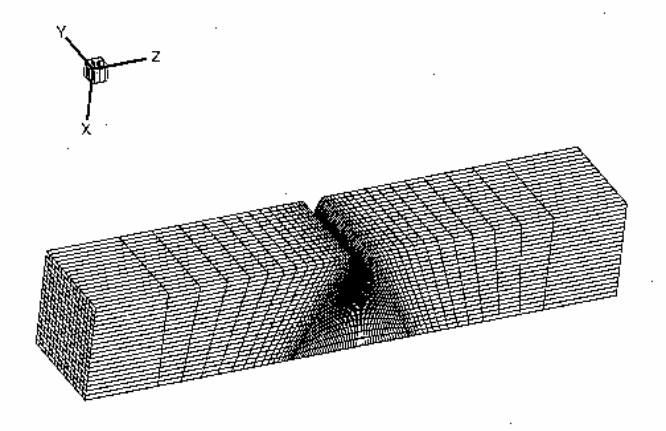

Figure 2: Finite element mesh for a 3D analysis.

In all calculations here, the initial void volume fraction is taken to be zero and void nucleation is specified by $\varepsilon_N = 0.3$, $f_N = 0.04$ and $s_N = 0.1$

Failure can occur either by microvoid nucleation, growth and coalescence or by cleavage. The material is partitioned into cleavage grains and it is assumed that cleavage failure in a grain occurs when the volume average of the maximum principal stress over that grain reaches a temperature and strain rate independent critical value σ_c , Tvergaard and Needleman [15]. In the calculations here, the cleavage grains are identified with the finite elements. In the region near the notch, where cleavage generally initiates, the variation in element size is not great but if substantial ductile crack growth occurs prior to cleavage, the high stress region involves larger elements which, because the stress average is taken over a larger volume, inhibits cleavage.

In the 3D analyses twenty node brick elements are used with eight point integration. The 3D mesh used to analyze the Charpy specimens is shown in Fig. 2. In the plane strain analyses to also be mentioned here, the simplest constant strain triangular elements are used, with the crossed triangle configuration for quadrilateral elements that is common in elastic-plastic analyses [16].

3 Numerical results

The weld geometries considered are specified according to Fig. 1 by taking $w_1 = 0.5\,mm$, $w_2 = 0.5\,mm$, and $w_3 = 8\,mm$. The location of the notch is specified by the value of x_c^2 in Fig. 1. For a case where the notch is parallel to the specimen surface Fig. 3 shows a numerical representation of the three material regions in two cases, for $x_c^2 = 0\ mm$, i.e. when the notch is in the centre of the weld material, and for $x_c^2 = 6.5\ mm$, when the notch tip is close to the more brittle HAZ. In Fig. 3 the base material is light grey, the weld material is darker grey, and the HAZ is black.

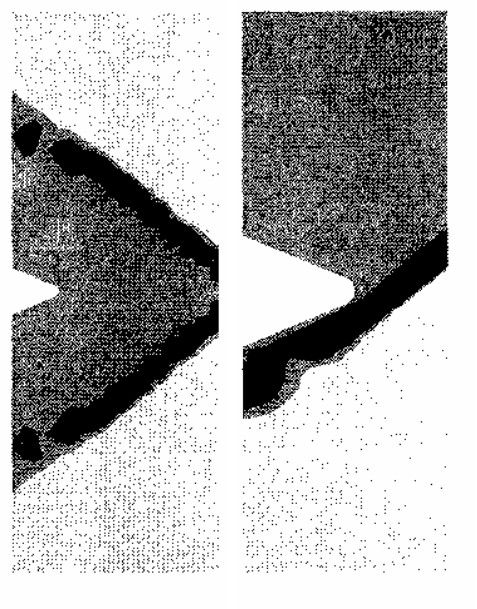

(a) (b)

Figure 3: Base material shown as light grey, weld material darker grey, and HAZ is black. (a) $x_c^2 = 0\ mm$. (b) $x_c^2 = 6.5\ mm$. (From [16]).

In a plane strain model of the Charpy specimen [16] the effect of the location of the notch has been analysed by varying the value of x_c^2 . The variation of the work to fracture shown in Fig. 4 illustrates clearly, for an overmatched as well as an undermatched weld that the most brittle response is found when x_c^2 is in the vicinity of the value 6.5 mm , i.e. when the failure starting from the notch tip will initiate in the brittle HAZ.

In a full 3D analysis for the overmatched material corresponding to the situation $x_c^2 = 6.5\ mm$ in Fig. 3b the effect of the specimen width has been investigated for an overmatched weld [17]. Where $C_0 = 10\ mm$ denotes the standard width of the Charpy V-notch specimen, the evolution of the maximum principal stress in the specimen has been investigated in [8] for plane strain and for 3D specimens with the thickness C_0 , $2C_0$ and $4C_0$. The somewhat surprising result was found that a full 3D analysis for the standard specimen gave more brittle behaviour than that predicted by the plane strain assumption, which has stronger constraint on the plastic deformation and also leads to higher force levels. Therefore, the 3D specimens with larger thickness were analysed to test possible convergence towards the plane strain result. The evolution of the maximum principal stress $\Sigma_{\max}$ (averaged over the element volume) is shown in Fig. 5 for a low temperature. Initially the peak stress is at the notch surface, but at the impacter displacement $U \cong 0.0004\ mm$ the curves show a kink, as the location of the maximum stress shifts to a point somewhat in front of the notch, where cleavage failure initiates when

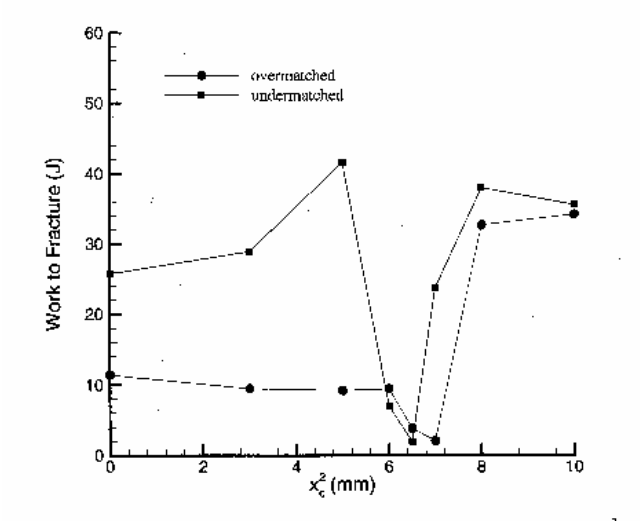

Figure 4: Work to fracture vs. location of the HAZ relative to the notch, as measured by the parameter x_c^2 , for two different materials. (From [16], but with the work of fracture multiplied by a factor of two to correct an error in [16] in calculating the work from the force-deflection curve).

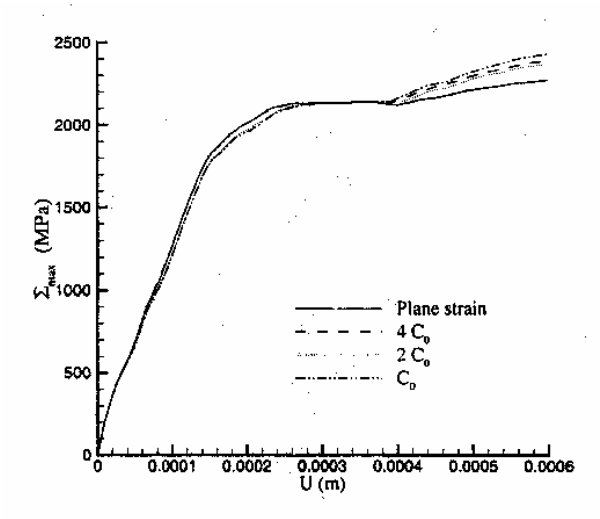

Figure 5: Evolution of the maximum principal stress with applied displacement for various values of the specimen thickness. C_0 is the thickness of the standard Charpy specimen. The weld configuration is that shown in Fig. 2b and the initial temperature is -80^oC . (From [17]).

$\Sigma_{\max}$ reaches a critical level. Fig. 4 shows that also for the specimens with larger thickness the peak stress remains well above that predicted for plane strain. The explanation found in [17] is that this stress peak occurs at a distance of about $C_0/2$ from the free surface at the specimen side, while the behaviour in the central part of the thick specimen has converged to the planar solution. For the specimen with the standard thickness C_0 the two edge regions of higher cleavage stress overlap into one central region.

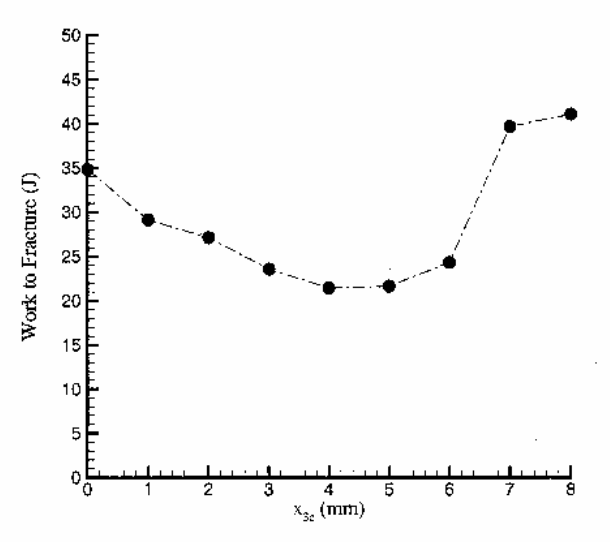

Figure 6: Work to fracture versus the location of the HAZ for a specimen with the notched surface rotated 90° from the surface of the welded piece. The notch location is measured by x_{3c} and the temperature is $\Theta_{\text{init}} = 0°\text{C}$. (From [18]).

The 3D analyses in [18] have also considered specimens as those in Fig. 3, with the notched surface parallel to the surface of the welded piece, and these studies for a much finer mesh have confirmed the result in [17] that strong three dimensional effects give much increased stress levels in the center of the specimen, which results in earlier onset of cleavage failure than predicted by plane strain analyses. However, the analyses in [18] have focussed mainly on the more complex geometries where the specimens are cut with the notched surface rotated 90° from the surface of the welded piece. In that case the geometry of the weld material on the notched surface of the Charpy specimen will look like the patterns shown in Fig. 1b and in Fig. 3. Thus, for notch locations inside the weld region the typical situation will be that at some point of the notch it crosses a thin material layer containing the more brittle HAZ. And when a crack grows ahead of the notch tip, the material in front of the same point of the notch will still be the more brittle HAZ, while the material in front of other parts of the notch will still be more ductile base material or weld material. The effect of the location of the notch on the work to fracture is illustrated in Fig. 6. As expected, the work to fracture is larger for $x_c^2 \geq 7\ mm$, i.e. when

the notch is so far removed from centre of the weld that the notch does not cross the HAZ, and a similar effect is seen when $x_c^2 = 0\ mm$, where the notch tip is in between two thin layers of HAZ. But the figure also shows that the smallest work to fracture occurs when the notch crosses the thin HAZ layer somewhere near the centre of the specimen, which is a result of the three dimensional nature of the stress field. As mentioned above, the principal stresses are larger near the centre, and therefore failure tends to occur earlier when the HAZ crosses the notch near the centre. As this crossing point moves closer to the free surfaces at the sides of the Charpy specimen the stress triaxiality level decreases and therefore the absorbed energy increases.

References

[1] A. A. Benzerga, V. Tvergaard, and A. Needleman. Size effects in the charpy v-notch test. *Int. J. Fract.*, 116:275–296, 2002.

[2] C. C. Chu and A. Needleman. Void nucleation effects in biaxially stretched sheets. *J. Engng. Mat. Tech.*, 102:249–256, 1980.

[3] D. Francois and A. Pineau. *From Charpy to Present Impact Testing.* Elsevier, Oxford, 2002.

[4] G. R. Gray and S.-R. Chen. Private communication, 1998.

[5] A. L. Gurson. *Plastic Flow and Fracture Behavior of Ductile Materials Incorporating Void Nucleation, Growth and Interaction.* PhD thesis, Brown University, 1975.

[6] K. K. Mathur, A. Needleman, and V. Tvergaard. 3D analysis of failure modes in the charpy impact test. *Modelling Simul. Mat. Sci. Engin.*, 2:617–635, 1994.

[7] J. Pan, M. Saje, and A. Needleman. Localization of deformation in rate sensitive porous plastic solids. *Int. J. Fract*, 21:261–278, 1983.

[8] R. O. Ritchie. On the relationship between fracture toughness and Charpy V-Notch Energy in ultrahigh strength steels. *in A.R. Rosenfield, H.L. Gegel, D.F. Hasson (eds.), What does the Charpy Test Really Tell Us, American Society for Metals*, pages 54–73, 1978.

[9] V. Tvergaard. Influence of voids on shear band instabilities under plane strain conditions. *Int. J. Fract.*, 17:389–407, 1981.

[10] V. Tvergaard. On localization in ductile materials containing spherical voids. *Int. J. Fract.*, 18:237–252, 1982.

[11] V. Tvergaard. Material failure by void growth to coalescence. *Adv. Appl. Mech.*, 27:83–151, 1990.

[12] V. Tvergaard and A. Needleman. Analysis of the cup-cone fracture in a round tensile bar. *Acta Metal.*, 32:157–169, 1984.

[13] V. Tvergaard and A. Needleman. Effect of material rate sensitivity on failure modes in the Charpy V-Notch test. *Int. J. Mech. Phys. Solids*, 34:213–241, 1986.

[14] V. Tvergaard and A. Needleman. An analysis of temperature and rate dependence of Charpy V-Notch energies for a high nitrogen steel. *Int. J. Fract.*, 37:197–215, 1988.

[15] V. Tvergaard and A. Needleman. An analysis of the brittle-ductile transition in dynamic crack growth. *Int. J. Fract.*, 59:53–67, 1993.

[16] V. Tvergaard and A. Needleman. Analysis of the Charpy V-Notch test for welds. *Engin. Frac. Mech.*, 65:627–643, 2000.

[17] V. Tvergaard and A. Needleman. 3D Charpy specimen analyses for welds. In D. Francois and A. Pineau., editors, *Charpy to Present Impact Testing*, pages 437–444, Elsevier, Oxford, 2002.

[18] V. Tvergaard and A. Needleman. 3D analyses of the effect of weld orientation in Charpy specimens. *Engng. Fracture Mechanics*, 71:2179–2195, 2004.